Supplementary Figure Legends and Tables Legends

Figure S1. Experimental setting of in vivo imaging studies.

Mice were inoculated subcutaneously with 1x10E7 ML-B7 or ML2-B15 control tumor cells in the right and left flank, respectively. After total body irradiation, 2x10E7 TCR2.5D6iRFP T_{CM}, 2x10E7 iRFP T_{CM} or PBS were injected intravenously. **(A)** Experimental setting for immuno-PET imaging. Mice received ^{89}Zr-labeled F(ab´)$_2$ and imaging was performed at day 5 followed by ex vivo analyses. **(B)** Investigation of the impact of F(ab´)$_2$ on T-cell function *in vivo*. Mice were injected intravenously with OKT11 (anti-CD2)-F(ab´)$_2$, T3-3A1 (anti-CD7)-F(ab´)$_2$ or isotype-F(ab´)$_2$. Tumor growth is monitored over 11 days followed by ex vivo analyses.

Figure S2. CD2, CD3 and CD7 are expressed on all T-cell subsets.

Flow cytometric analysis of CD2, CD3 and CD7 expression on the surface of different T-cell subsets from freshly isolated peripheral blood mononuclear cells (PBMC). **(A)** Expression on CD4$^+$ T-cell subpopulations. CD3$^+$ cells were gated on CD4$^+$ cells and analyzed for the single T-cell subpopulations naïve T cells (T_N; CD45RA$^+$CD62L$^+$), central memory T cells (T_{CM}; CD45RA$^-$ CD62L$^+$), effector memory T cells (T_{EM}; CD45RA$^-$CD62L$^-$), effector T cells (T_{EFF}; CD45RA$^+$CD62L$^-$) and regulatory T cells (T_{Reg}; CD127$^-$CD25$^+$) (left side). Respective histograms of T-cell subpopulation staining with PE-labeled anti-CD2, anti-CD3, anti-CD7 and PE-isotype control antibodies are shown on the right side. **(B)** Expression on CD8$^+$ T-cell subpopulations. As described above, CD3$^+$ cells were gated on CD8 and then analyzed for the respective T-cell subpopulations (left side). Histograms show the respective expression of CD2, CD3 and CD7 (right side).

Figure S3. Expression of CD2, CD7 and CD3 on different subsets of freshly isolated PBMC.

Mean fluorescence intensity (MFI) values of CD2 (left panel), CD3 (middle panel) and CD7 (right panel) expression on various subsets of peripheral mononuclear blood cells (PBMC). Therefore, 7-AAD$^-$ pre-gated cells were analyzed for monocytes (CD33$^+$CD14$^+$), B cells (CD20$^+$), NK cells

($CD56^+$) and NK T cells ($CD3^+CD56^+$). The experiment was performed with blood cells from three different donors (n=3) and the results of one representative experiment are shown.

Figure S4. Anti-CD3, but not anti-CD2 and anti-CD7 antibodies induce apoptosis of PBMC-derived T cells *in vitro* with correspondingly high IFNγ production.

PBMC-derived T cells were incubated with different antibody concentrations for 18h. OKT3 served as positive control. Data are shown as mean ± standard deviation (sd) from triplicates. One representative of three performed experiments is shown (n=3). **(A)** Percentage of apoptotic cells (Annexin5 or 7-AAD positive) after incubation at various concentrations of depicted antibodies. **(B)** Corresponding IFNγ levels in supernatant of incubated cells.

Figure S5. SE-HPLC analysis of OKT11 (anti-CD2) and T3-3A1 (anti-CD7) IgG and F(ab´)$_2$ revealed one subclass (IgG1) for OKT11 (anti-CD2) and two subclasses (IgG1, IgG2a) for T3-3A1 (anti-CD7), both specific for CD7.

(A) SE-HPLC analysis for OKT11 (anti-CD2) and T3-3A1 (anti-CD7) IgG and F(ab´)$_2$. **(B)** Optical density (OD) of isotype subclasses from analysis of OKT11 (anti-CD2)-IgG (left panel) and T3-3A1 (anti-CD7)-IgG (right panel) by ELISA. **(C)** Flow cytometry plots for binding of T3-3A1 (anti-CD7)-IgG mixture (IgG1/IgG2a) to T cells with and without preceding blocking of the CD7 antigen by a sheep anti-human CD7 antibody. Cells were stained for bound IgG1 (left panel) and IgG2a (middle panel). OKT3 (anti-CD3)-IgG (IgG2a) served as negative control for blocking of IgG1 and OKT11 (anti-CD2)-IgG (IgG1) for blocking of IgG2a. Specificity of the sheep anti-human CD7 antibody was confirmed by secondary staining with anti-sheep antibody (right panel).

Figure S6. Selected OKT11 (anti-CD2) and T3-3A1 (anti-CD7) IgG and respective F(ab´)$_2$ do not induce IFNγ release.

PBMC-derived T cells were incubated for 72 h at 37 °C with 100 nM of indicated IgG and F(ab´)$_2$. Incubation with isotypes served as negative control and OKT3 (anti-CD3)-IgG as positive control. IFNγ secretion detected in the supernatant is shown as mean ± sd from triplicates (n=3).

Figure S7. T3-3A1 (anti-CD7) IgG as well as F(ab´)$_2$ do not induce IFNγ release nor proliferation at different dose levels *in vitro*.

(A) IFNγ release of PBMC-derived T cells after 18 h of co-cultivation with the indicated IgG and F(ab´)$_2$ at depicted concentrations. Respective isotypes and OKT3 (anti-CD3)-IgG served as controls. Mean ± sd is depicted (n=3). **(B)** Plots on MFI of CTV stained cells after incubation with different dose levels of tested IgG, F(ab´)$_2$ and controls. **(C)** Corresponding IFNγ release at depicted time points.

Table S1. Percentage of CD2, CD3 and CD7 expressing cells on CD4$^+$ T-cell subpopulations.

The percentages of CD3$^+$ of all cells alive, CD4$^+$ of CD3$^+$ cells and T-cell subpopulations on CD4$^+$ cells are presented as mean ± sd from all analyzed samples. The single T-cell subpopulations are naïve T cells (T_N; CD45RA$^+$CD62L$^+$), central memory T cells (T_{CM}; CD45RA$^-$CD62L$^+$), effector memory T cells (T_{EM}; CD45RA$^-$CD62L$^-$), effector T cells (T_{EFF}; CD45RA$^+$CD62L$^-$) and regulatory T cells (T_{Reg}; CD4$^+$CD25$^+$CD127^{low}). Moreover, the percentage of CD2$^+$, CD3$^+$ and CD3$^+$cells for different T-cell subsets is depicted.

Table S2. Percentage of CD2, CD3 and CD7 expressing cells on CD8$^+$ T-cell subpopulations.

As described for Table S2, the percentages of CD3$^+$ of all cells alive, CD8$^+$ of CD3$^+$ cells and T-cell subpopulations on CD8$^+$ cells are presented as mean ± sd from all analyzed samples. The single T-cell subpopulations are naïve T cells (T_N; CD45RA$^+$CD62L$^+$), central memory T cells (T_{CM}; CD45RA$^-$CD62L$^+$), effector memory T cells (T_{EM}; CD45RA$^-$CD62L$^-$) and effector T cells (T_{EFF};

CD45RA^{+}CD62L^{-}). Besides, the percentage of CD2^{+}, CD7^{+} and CD3^{+} cells for different T-cell subsets is depicted.

Table S3. Biodistribution results of in vivo T-cell imaging at the specific tumor site by immuno-PET using ^{89}Zr-OKT11 (anti-CD2)-F(ab´)$_2$.

The percentage injected dose per gram (%ID/g) of the depicted organs from animals injected with TCR2.5D6iRFP T_{CM} (n=3) or PBS (n=1) and receiving ^{89}Zr-OKT11 (anti-CD2)-F(ab´)$_2$ is shown for each animal as well as mean ± sd for the TCR2.5D6iRFP T_{CM} injected mice.

Table S4. Biodistribution results of in vivo T-cell imaging at the specific tumor site by immuno-PET using ^{89}Zr-T3-3A1 (anti-CD7)-F(ab´)$_2$.

%ID/g of different organs from animals injected with TCR2.5D6iRFP T_{CM} (n=3) or PBS (n=1) and receiving ^{89}Zr-T3-3A1 (anti-CD7)-F(ab´)$_2$is shown for each animal as well as mean ± sd for the TCR2.5D6iRFP T_{CM} injected mice.

Table S5. Biodistribution results of in vivo T-cell imaging at the specific tumor site by immuno-PET using ^{89}Zr-T3-3A1 (anti-CD7)-F(ab´)$_2$.

The table depicts %ID/g of ex vivo analysis of different organs from animals injected with TCR2.5D6iRFP T_{CM} (n=7) or iRFP T_{CM} (n=6) which all received ^{89}Zr-T3-3A1 (anti-CD7)-F(ab´)$_2$. Data of each animal as well as mean ± sd for the groups is shown.

Figure S1

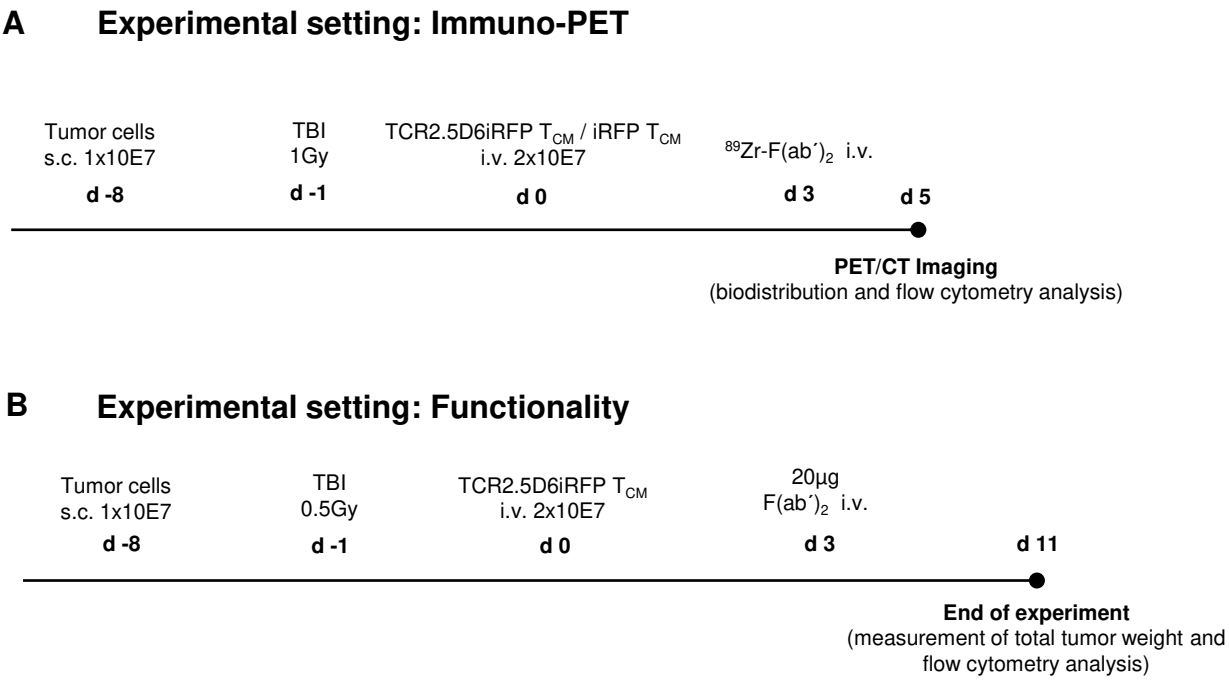
A
Experimental setting: Immuno-PET
Tumor cells
s.c. 1x10E7
d -8
TBI
1Gy
d -1
TCR2.5D6iRFP T_CM / iRFP T_CM
i.v. 2x10E7
d 0
89Zr-F(ab´)2 i.v.
d 3
d 5
PET/CT Imaging
(biodistribution and flow cytometry analysis)
B
Experimental setting: Functionality
Tumor cells
s.c. 1x10E7
d -8
TBI
0.5Gy
d -1
TCR2.5D6iRFP T_CM
i.v. 2x10E7
d 0
20µg
F(ab´)2 i.v.
d 3
d 11
End of experiment
(measurement of total tumor weight and
flow cytometry analysis)

Figure S2

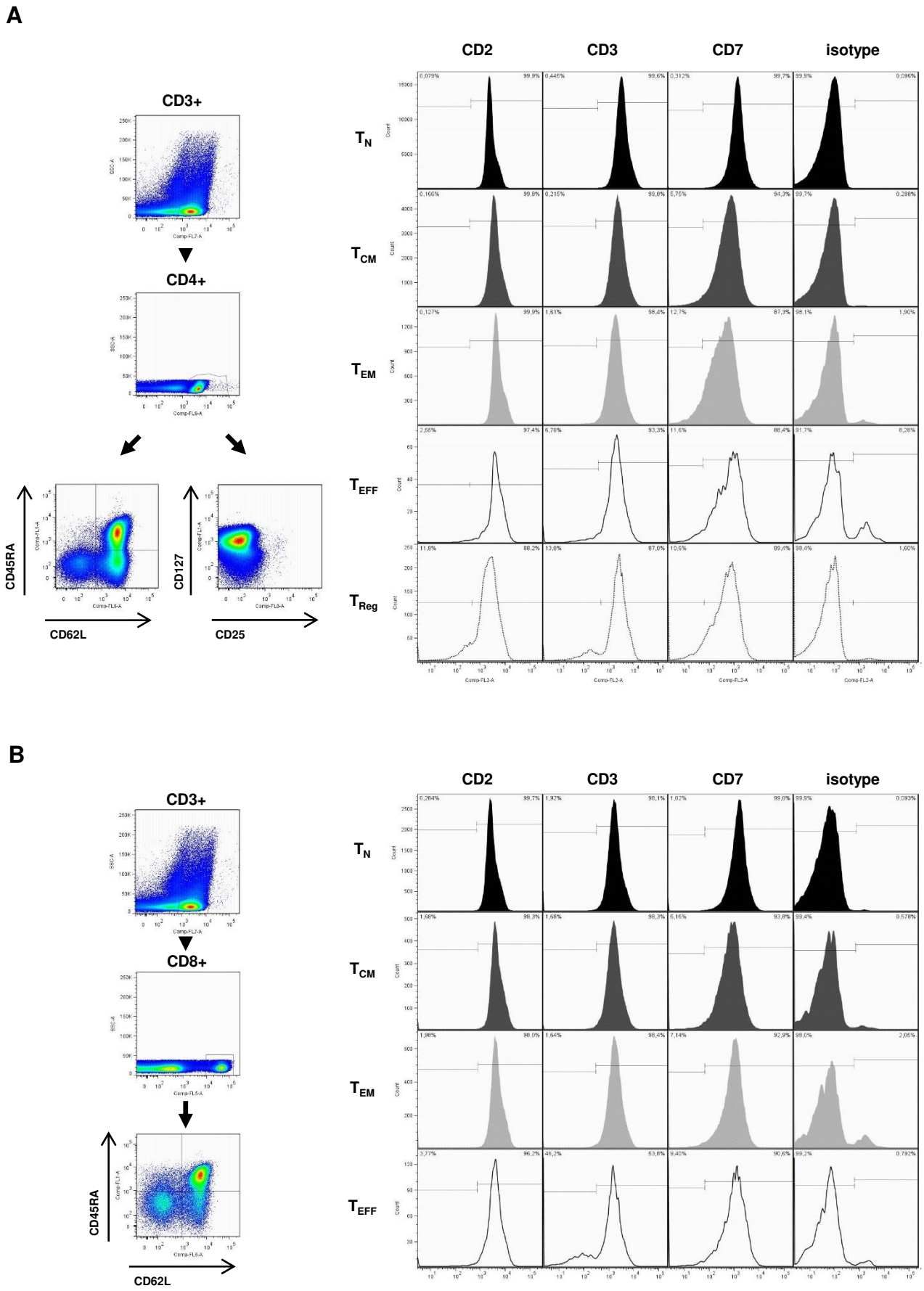
A
CD3+
CD4+
CD45RA
CD62L
CD127
CD25
CD2
CD3
CD7
isotype
T_N
T_CM
T_EM
T_EFF
T_Reg
B
CD3+
CD8+
CD45RA
CD62L
CD2
CD3
CD7
isotype
T_N
T_CM
T_EM
T_EFF

Figure S3

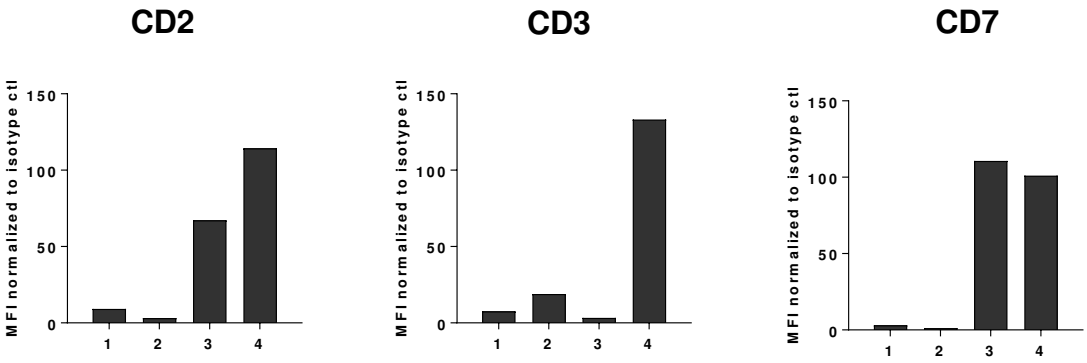

1 monocytes ($CD33^{+}CD14^{+}$)

2 B cells ($CD20^{+}$)

3 NK cells ($CD56^{+}$)

4 NK T cells ($CD56^{+}CD3^{+}$)

Figure S4

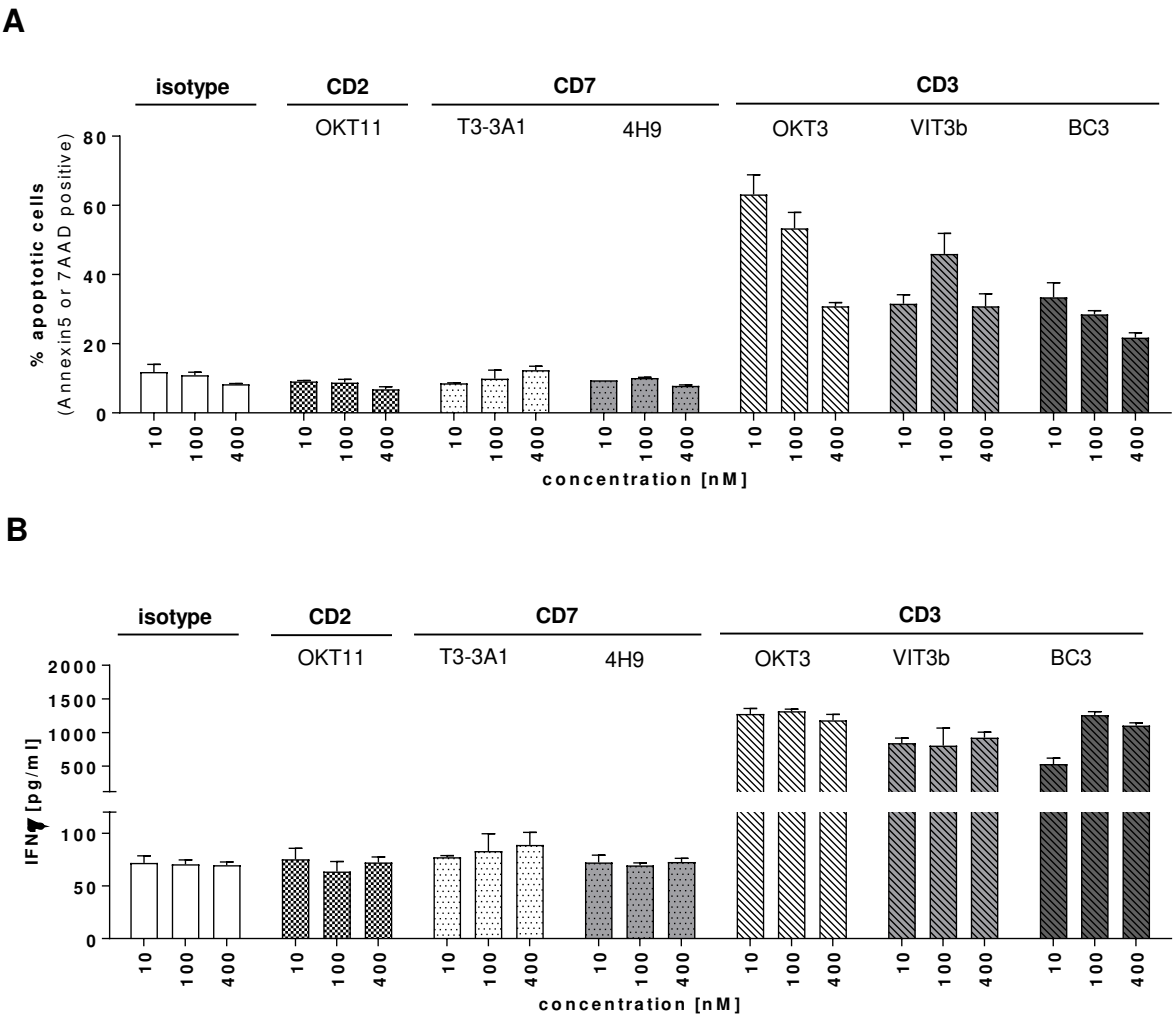
A
isotype
CD2
CD7
CD3
OKT11
T3-3A1
4H9
OKT3
VIT3b
BC3
% apoptotic cells
(Annexin5 or 7AAD positive)
0
20
40
60
80
10
100
400
concentration [nM]
B
isotype
CD2
CD7
CD3
OKT11
T3-3A1
4H9
OKT3
VIT3b
BC3
IFNγ [pg/ml]
0
50
100
500
1000
1500
2000
10
100
400
concentration [nM]

Figure S5

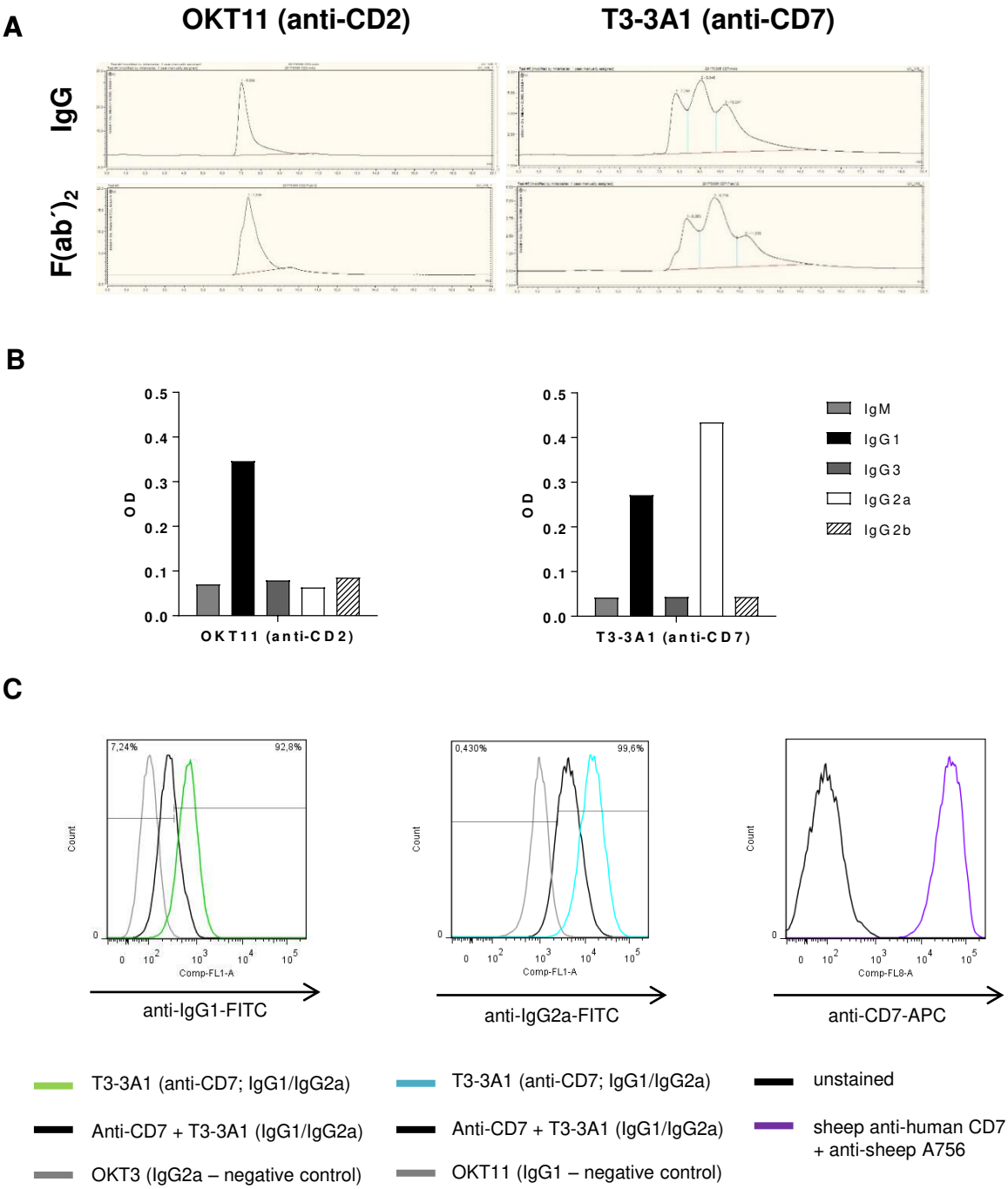
A
OKT11 (anti-CD2)
T3-3A1 (anti-CD7)
IgG
F(ab´)2
B
OD
0.5
0.4
0.3
0.2
0.1
0.0
OKT11 (anti-CD2)
T3-3A1 (anti-CD7)
IgM
IgG1
IgG3
IgG2a
IgG2b
C
7,24%
92,8%
0,430%
99,6%
Count
Comp-FL1-A
Comp-FL8-A
anti-IgG1-FITC
anti-IgG2a-FITC
anti-CD7-APC
T3-3A1 (anti-CD7; IgG1/IgG2a)
Anti-CD7 + T3-3A1 (IgG1/IgG2a)
OKT3 (IgG2a – negative control)
T3-3A1 (anti-CD7; IgG1/IgG2a)
Anti-CD7 + T3-3A1 (IgG1/IgG2a)
OKT11 (IgG1 – negative control)
unstained
sheep anti-human CD7
+ anti-sheep A756

Figure S6

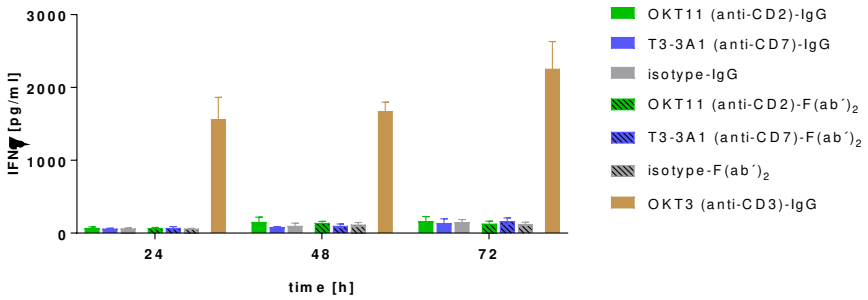
3000
2000
1000
0
IFNγ [pg/ml]
24
48
72
time [h]
OKT11 (anti-CD2)-IgG
T3-3A1 (anti-CD7)-IgG
isotype-IgG
OKT11 (anti-CD2)-F(ab´)2
T3-3A1 (anti-CD7)-F(ab´)2
isotype-F(ab´)2
OKT3 (anti-CD3)-IgG

Figure S7

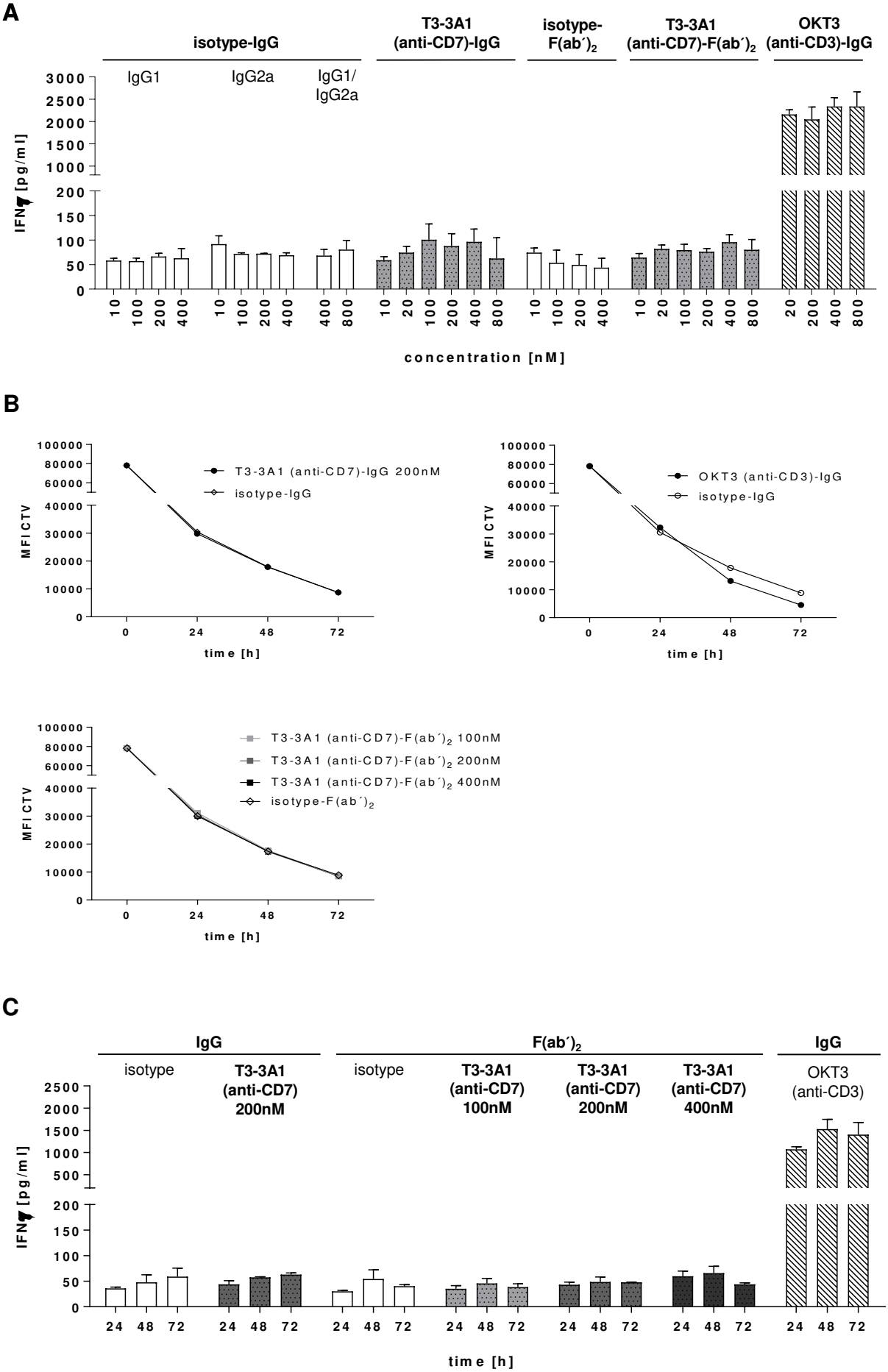
A
isotype-IgG
T3-3A1 (anti-CD7)-IgG
isotype-F(ab´)2
T3-3A1 (anti-CD7)-F(ab´)2
OKT3 (anti-CD3)-IgG
IgG1
IgG2a
IgG1/ IgG2a
IFNγ [pg/ml]
concentration [nM]
B
T3-3A1 (anti-CD7)-IgG 200nM
isotype-IgG
OKT3 (anti-CD3)-IgG
isotype-IgG
T3-3A1 (anti-CD7)-F(ab´)2 100nM
T3-3A1 (anti-CD7)-F(ab´)2 200nM
T3-3A1 (anti-CD7)-F(ab´)2 400nM
isotype-F(ab´)2
MFI CTV
time [h]
C
IgG
F(ab´)2
IgG
isotype
T3-3A1 (anti-CD7) 200nM
isotype
T3-3A1 (anti-CD7) 100nM
T3-3A1 (anti-CD7) 200nM
T3-3A1 (anti-CD7) 400nM
OKT3 (anti-CD3)
IFNγ [pg/ml]
time [h]

Table S1

CD3+ (68,6 ± 2,3%/all cells alive)				
CD4+ (74,3 ± 8,5%/CD3+)	**CD2+**	**CD3+**	**CD7+**	**isotype**
T_N (67,3 ± 2,8%/CD4+)	99,9%	99,6%	99,7%	0,1%
T_{CM} (24,8 ± 2,3%/CD4+)	99,8%	99,8%	94,3%	0,3%
T_{EM} (7,3 ± 0,7%/CD4+)	99,9%	98,4%	87,3%	1,9%
T_{EFF} (0,7 ± 0,2%/CD4+)	97,3%	93,3%	88,4%	8,3%
T_{Reg} (1,4 ± 0,2%/CD4+)	88,2%	87,0%	89,4%	1,6%

Table S2

$CD3^+$ (68,6 ± 2,3%/all cells alive)				
$CD8^+$ (16,0 ± 2,1%/$CD3^+$)	**$CD2^+$**	**$CD3^+$**	**$CD7^+$**	**isotype**
T_N (64,3 ± 2,3%/$CD4^+$)	99,7%	98,1%	99,0%	0,1%
T_{CM} (13,3 ± 1,9%/$CD4^+$)	98,3%	98,3%	93,8%	0,6%
T_{EM} (17,7 ± 1,1%/$CD4^+$)	98,0%	98,4%	92,9%	2,1%
T_{EFF} (4,8 ± 0,8%/$CD4^+$)	96,2%	53,8%	90,6%	0,8%

Table S3

^{89}Zr-OKT11 (anti-CD2)-F(ab´)$_2$	2.5D6iRFP T_{CM}				PBS
%ID/g	1	2	3	mean ± sd	1
ML2-B7	21,11	8,27	9,36	12,91 ± 5,81	3,81
ML2-B15	2,76	2,60	3,02	2,80 ± 0,17	3,34
spleen	27,87	36,81	31,79	32,15± 3,66	14,24
liver	9,38	10,11	8,07	9,19 ± 0,84	8,17
lung	7,76	7,10	3,87	6,24 ± 1,70	4,70
kidney	42,92	38,49	23,57	34,99 ± 8,28	56,48
muscle	1,08	0,81	0,92	0,93 ± 0,11	1,23
blood	4,38	3,42	3,80	3,87 ± 0,39	6,65

Table S4

^{89}Zr-T3-3A1 (anti-CD7)-F(ab´)$_2$	2.5D6iRFP T_{CM}				PBS
%ID/g	1	2	3	mean ± sd	1
ML2-B7	13,31	13,65	8,87	11,93 ± 2,18	1,95
ML2-B15	3,23	2,42	1,78	2,48 ± 0,59	1,93
spleen	22,19	19,29	13,92	18,46 ± 3,43	8,17
liver	7,24	6,94	5,58	6,59 ± 0,72	4,91
lung	4,87	3,64	2,98	3,83 ± 0,78	2,06
kidney	65,19	49,37	32,31	48,96 ± 13,43	29,86
muscle	1,44	0,49	0,57	0,83 ± 0,43	0,71
blood	2,29	1,99	1,47	1,92 ± 0,34	1,63

Table S5

^{89}Zr-T3-3A1 (anti-CD7)-F(ab´)$_2$															
	2.5D6iRFP TCM								iRFP TCM						
%ID/g	1	2	3	4	5	6	7	mean ± sd	1	2	3	4	5	6	mean ± sd
ML2-B7	2,02	1,92	1,89	1,67	1,93	1,78	2,37	1,94 ± 0,20	2,06	2,13	2,16	1,60	1,45	1,58	1,83 ± 0,29
ML2-B15	18,63	11,92	11,72	13,57	11,97	12,20	13,61	13,37 ± 2,27	10,30	15,58	18,74	13,49	10,76	7,96	12,80 ± 3,59
spleen	6,28	5,56	5,63	6,27	5,26	4,55	6,05	5,66 ± 0,57	5,08	6,62	7,75	4,97	4,17	4,18	5,46 ± 1,31
liver	2,87	3,38	3,23	3,35	1,94	2,06	2,45	2,75 ± 0,56	2,33	2,49	3,15	1,86	1,52	1,42	2,13 ± 0,60
lung	42,72	44,13	44,82	46,16	19,41	24,64	31,23	36,16 ± 10,14	40,57	45,11	55,54	18,43	23,26	19,91	33,80 ± 14,06
kidney	0,56	0,67	0,56	0,58	0,52	0,56	0,65	0,59 ± 0,05	0,80	0,61	1,45	0,52	0,63	0,53	0,76 ± 0,32
muscle	2,70	2,68	2,88	2,37	2,19	2,27	2,68	2,54 ± 0,24	2,73	2,95	3,49	2,05	1,83	1,77	2,47 ± 0,63
blood	2,02	1,92	1,89	1,67	1,93	1,78	2,37	1,94 ± 0,20	2,06	2,13	2,16	1,60	1,45	1,58	1,83 ± 0,29